Surface Wave Reduction in Antenna Arrays Using Metasurface Inclusion for MIMO and SAR Systems

Mohammad Alibakhshikenari[1]*, Bal S. Virdee[2], Chan H. See[3,4], Raed A. Abd-Alhameed[5], Francisco Falcone[6], and Ernesto Limiti[1]

[1] Electronic Engineering Department, University of Rome "Tor Vergata", Via del Politecnico 1, 00133, Rome, ITALY
[2] London Metropolitan University, Center for Communications Technology & Mathematics, School of Computing & Digital Media, London N7 8DB, UK
[3] School of Eng. & the Built Environment, Edinburgh Napier University, 10 Colinton Rd., Edinburgh, EH10 5DT, UK
[4] School of Engineering, University of Bolton, Deane Road, Bolton, BL3 5AB, UK
[5] Faculty of Engineering and Informatics, University of Bradford, Bradford, BD7 1DP, UK
[6] Electrical and Electronic Engineering Department, Public University of Navarre, 31006 Pamplona, SPAIN
*alibakhshikenari@ing.uniroma2.it

Abstract- **An effective method is presented for suppressing mutual coupling between adjacent radiating elements which is based on metasurface isolation for MIMO and synthetic aperture radar (SAR) systems. This is achieved by choking surface current waves induced over the patch antenna by inserting a cross-shaped metasurface structure between the radiating elements. Each arm of the cross-shaped structure constituting the metasurface is etched with meander-line slot (MLS). Effectiveness of the metasurface is demonstrated for a 2×2 antenna array that operates over six frequency sub-bands in X, Ku and K-bands. With the proposed technique, the maximum improvement achieved in attenuating mutual coupling between neighbouring antennas is: 8.5 dB (8-8.4 GHz), 28 dB (9.6-10.8 GHz), 27 dB (11.7-12.6 GHz), 7.5 dB (13.4-14.2 GHz), 13 dB (16.5-16.8 GHz) and 22.5 dB (18.5-20.3 GHz). Furthermore, with the proposed technique (i) minimum center-to-center separation between the radiating elements can be reduced to $0.26\lambda_0$, where λ_0 is 8.0 GHz; (ii) use of ground-plane or defected ground structures are unnecessary; (iii) use of short-circuited via-holes are avoided; (iv) it eliminates the issue with poor front-to-back ratio; and (v) it can be applied to existing arrays retrospectively.**

Keywords- **Metasurface isolator, MIMO, synthetic-aperture radar, Meander line slot (MLS), Mutual coupling, Antenna array.**

I. INTRODUCTION

Minimum spacing between the radiating elements of $0.5\lambda_0$ is normally required for achieving acceptable isolation between elements in microstrip MIMO antenna arrays. Otherwise the antenna performance is compromised in terms of radiation efficiency, gain and bandwidth due to the increased electromagnetic (EM) coupling among the closely packed antenna elements resulting from near-field effects [1]. Antenna arrays are important in next generation wireless communications systems such as 5G for beam steering and mitigating multipath fading.

Various techniques have been previously explored to reduce mutual coupling between two neighbouring patches, e.g. by integrating electromagnetic band-gap (EBG) structures in patch antenna arrays [2]-[4] or implementing defected ground structures (DGS) in the ground-plane [5][6]. Although these techniques are effective in reducing mutual coupling, however the minimum edge-to-edge spacing between adjacent elements needs to be $0.5\lambda_0$. Waveguided metamaterial is another relatively recent stopband technique [7] realized by etching metamaterial unit-cells in the ground-plane under a microstrip-line to enhance the current paths in the ground. With this technique edge-to-edge element spacing of $0.125\lambda_0$ can be achieved and the reduction in coupling is confined to only one plane; however, with this approach the impedance bandwidth is limited to 0.02 GHz.

This research work describes a new technique to substantially reduce EM coupling between adjacent radiating elements with reduced centre-to-centre spacing of $0.26\lambda_0$, where λ_0 is at 8.0 GHz. This is achieved by implementing a metasurface consisting of meander-line slot etched inside a microstrip structure, which is inserted between neighbouring patches [8]-[11]. The proposed metasurface minimises the effects of EM coupling resulting from space-wave and the near-field. Compared to other techniques reported in literature, the proposed technique reduces the fabrication process because no ground-plane defection or short-circuited via-holes are required; and it eliminates the issue with poor front-to-back ratio. The effectiveness of the proposed technique is validated with measured results. The proposed technique is applied on a wideband antenna operating in X, Ku and K bands. In X-band the application of the antenna is for military communication and wideband global satellite communication systems (WGS), in the Ku-band it is for terrestrial microwave and radar, specially police traffic speed-detector and in the K-band it is for airport surface detection equipment (ASDE).

II. METASURFACE ISOLATOR

The proposed two-dimensional metasurface isolator is constituted by etching a meander-line slot (MLS) on a microstrip structure. In Figs. 1 and 2, the cross-shaped metasurface is incorporated between adjacent radiating patches in a 2×2 antenna array that has a truncated ground-plane. The proposed metasurface essentially chokes surface current waves induced over the antenna by near-field effects thus minimising EM coupling between the radiating elements. Although not shown the ground planes are common. The antenna array was constructed using a standard PCB etching technique on FR-4 dielectric substrate with relative permittivity of 4.3, thickness of 1.6 mm and loss-tangent of 0.025. The square patch has dimensions of 15×15 mm² and the gap between the patch elements is 10 mm.

(a)   (b)   (c)
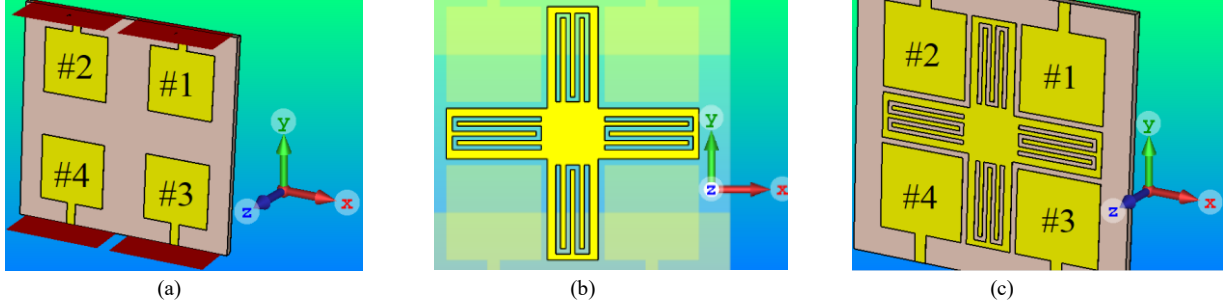
Fig. 1. Geometry of the antenna array and proposed metasurface. (a) Reference MIMO 2×2 antenna array without metasurface isolator; (b) Proposed metasurface isolator implemented using MLS; and (c) Antenna array with metasurface isolator.

The proposed antenna structure in Fig. 1 was analysed using CST-Microwave Studio EM solver, where open (Add Space) boundary condition was applied to create a realistic model. Dimensions of the 2×2 antenna array were optimized using CST Microwave Studio to realize maximum bandwidth in the operating frequency bands. Dimensions of the MLS were optimized to realize high isolation between adjacent patches but without significantly affecting the antenna's return-loss performance. The length and width of the arms of the cross-shaped isolator are 18.7 mm and 10.2 mm, respectively. It was observed that the most sensitive part of the proposed MLS to realise high isolation is its length of 69.9 mm and width of 0.57 mm. MLS is not implemented in the central section of the cross-shaped isolator because it facilitates electromagnetic interaction with the MLS arms of the cross-shaped structure, thus adversely affecting mutual coupling suppression and therefore the antenna's bandwidth, isolation, and radiation properties.
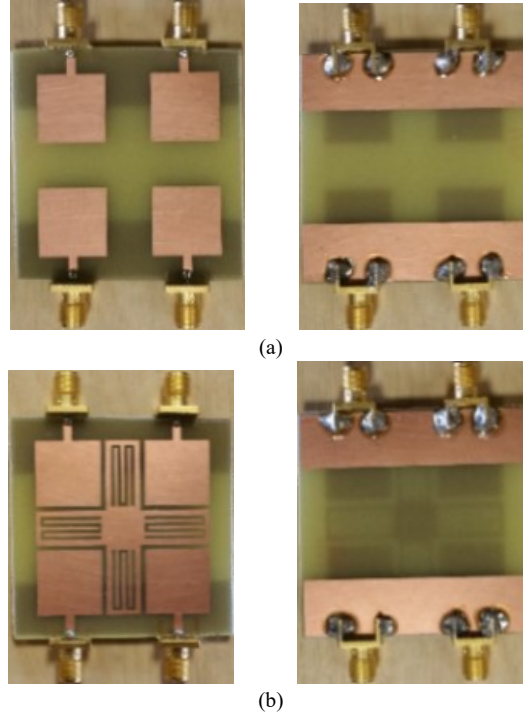

(a)

(b)

Fig. 2. (a) Fabricated prototypes of the antenna array without metasurface isolator (front & back), and (b) Fabricated prototypes with metasurface isolator (front & back). Length & width of each patch is 15 mm, and gap between them is 10 mm. Length & width of the meander line metasurface is 69.9 mm & 0.57 mm, respectively.

Figs. 3-5 show the transmission and reflection-coefficients of two identical 2×2 antenna arrays, where the reference antenna array has no metasurface. These two parameters were measured using a network analyser. It is evident that the antenna array with

the metasurface exhibits greater isolation than the reference antenna array in the six operating sub-bands defined for $|S_{11}| \leqq -10$ dB. This is because the metasurface suppresses propagation of surface waves over the antenna and compensates the otherwise out-of-phase radiation from the microstrip patch antennas to improve its reflection-coefficient performance. Improvement in the isolation is given in Table I. It is also evident in Figs. 3-5 there is general improvement in the reflection-coefficient too.
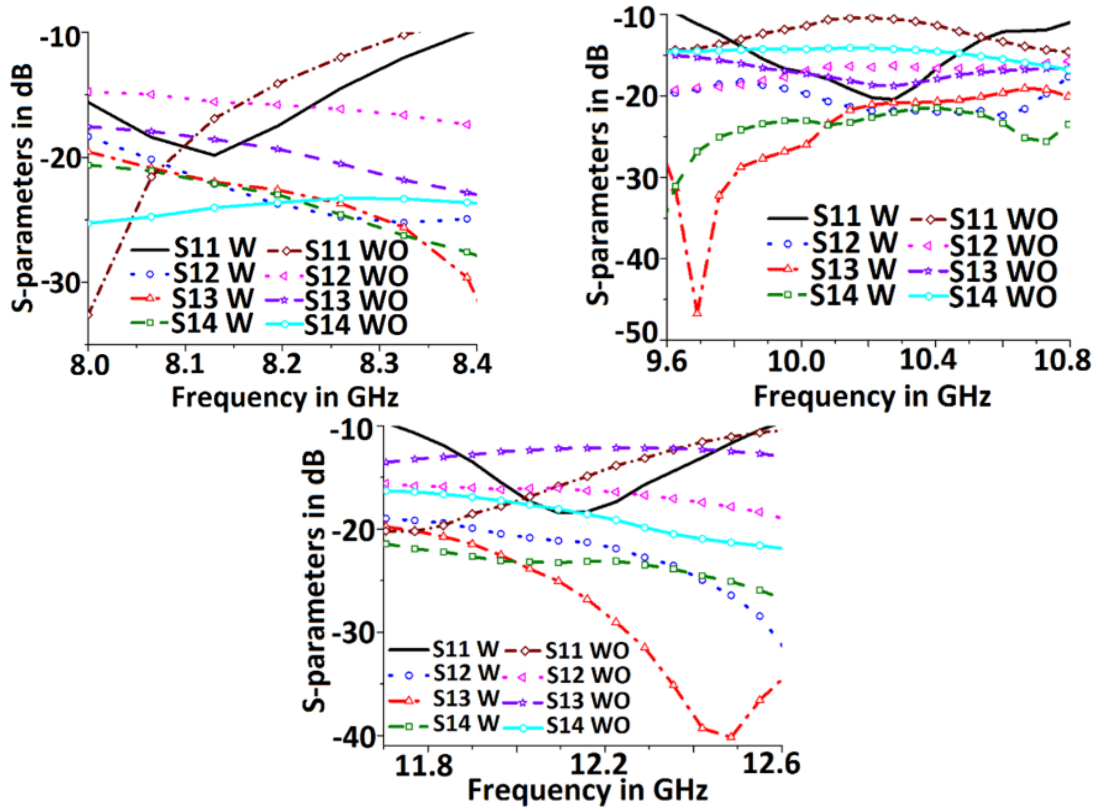

Fig. 3. Measured reflection & transmission-coefficient responses with (W) and without (WO) metasurface isolator at X- and Ku-bands.
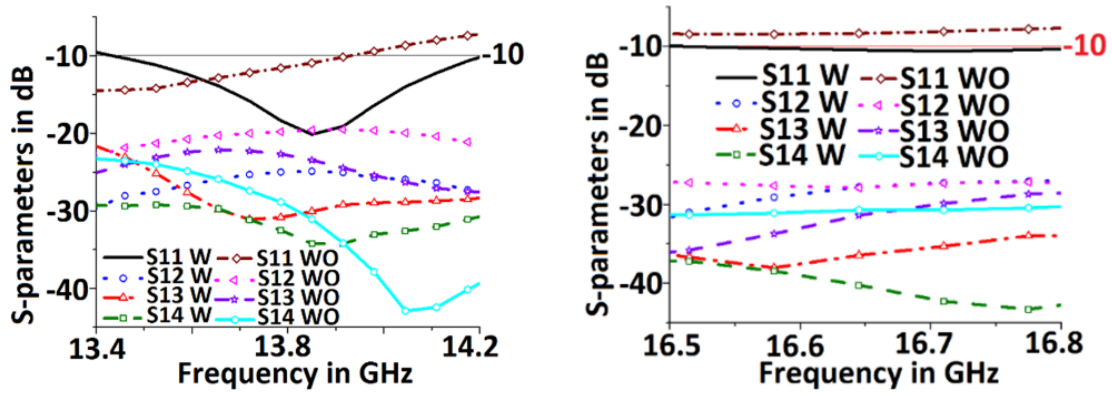

Fig. 4. Measured reflection & transmission-coefficient responses with (W) and without (WO) metasurface isolator at Ku-band.
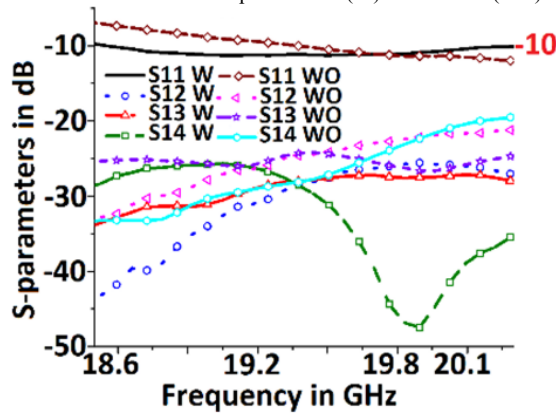

Fig. 5. Measured reflection & transmission-coefficient responses with (W) and without (WO) metasurface isolator at K-band.

TABLE I. ISOLATION IMPROVEMENT WITH METASURFACE

Freq. range (GHz)	$|S_{12}|$ (dB) Min./Max./Ave.	$|S_{13}|$ (dB) Min./Max./Ave.	$|S_{14}|$ (dB) Min./Max./Ave.
1: 8-8.4	7.5 / 8.5 / 8	2 / 8.5 / 6	- / 3 / -
2: 9.6-10.8	2.5 / 3.5 / 3	5 / 28 / 17	7 / 18 / 12.5
3: 11.7-12.6	3.5 / 13 / 9.5	8 / 27 / 18	5 / 5 / 5
4: 13.4-14.2	5.5 / 7.5 / 6.5	- / 4 / 2	- / 6.5 / 3.5
5: 16.5-16.8	- / 3.5 / 2	2 / 5.5 / 4	7 / 13 / 10.5
6: 18.5-20.3	4.5 / 22.5 / 13.5	2.5 / 7.5 / 5.5	5.5 / 20 / 13

The equivalent electrical circuit model of the antenna is shown in Fig. 6 where the patch radiator is represented with a resonant circuit comprising inductance L_P, capacitance C_P, and resistance R_P; and where MLS is represented by inductance L_M and capacitance C_M, whose magnitude depends on the gap between the radiators. Coupling between the patch and metasurface isolator is through a combination of L_C and C_C. Inductance L_C is more dominant because the metasurface isolator is coupled via non-radiating edge of the patch antenna. Ohmic and dielectric loss associated with the metasurface isolator is modelled by resistance R_M. Optimised values of the equivalent circuit model given in Table II were extracted using Keysight's ADS software tool based on S-parameter curves obtained from CST Microwave Studio. The equivalent circuit model was used to determine the effectiveness of the metasurface on the antenna array's return-loss and isolation performance. To validate this circuit model, its input impedance was computed using CST Microwave Studio and equivalent circuit model (CM), which are shown in Fig. 7.
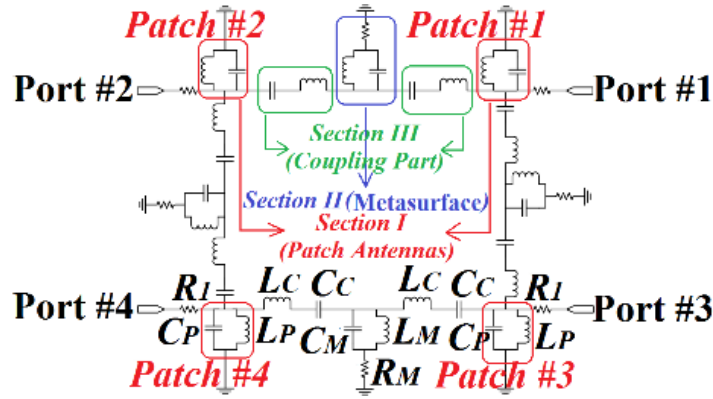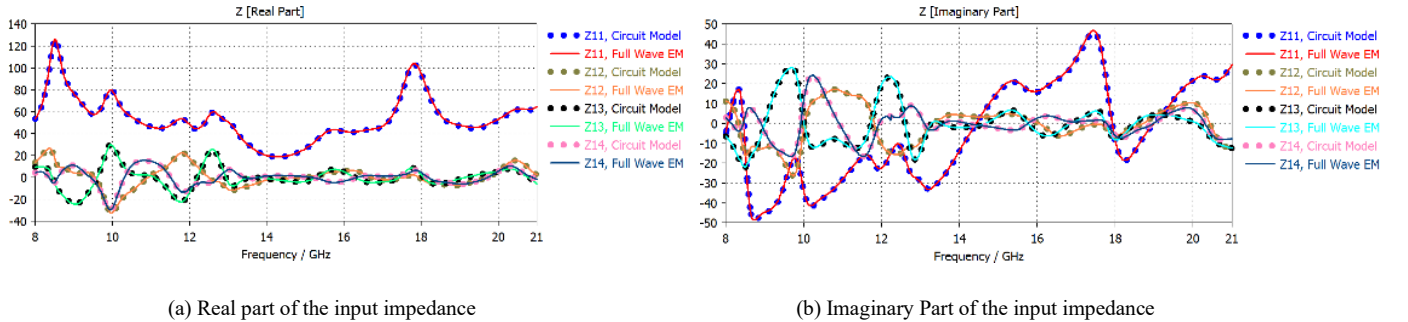

Fig. 6. Equivalent circuit diagram of the proposed antenna array.

TABLE II. OPTIMIZED VALUES OF THE EQUIVALENT MODEL REPRESENTING THE PROPOSED STRUCTURE

C_P	L_P	R_P	C_M	L_M	R_M	C_C	L_C	R_I
1.0 pF	7.1 nH	50 Ω	5.5 pF	2.8 nH	70 Ω	8.1 pF	0.7 nH	75.5 Ω

(a) Real part of the input impedance

(b) Imaginary Part of the input impedance

Fig. 7. Input impedance (Ω) of the proposed antenna array obtained using EM simulation and equivalent circuit model.

4

Radiation patterns of the 2×2 antenna array were measured in a standard anechoic chamber by exciting all four elements simultaneously in-phase. Fig. 8 shows the simulated and measured radiation characteristics in the vertical plane of the array with and without the metasurface isolator at selected spot frequencies of 8.15, 10.3, 12.15, 13.9, 16.7, and 19.9 GHz across the operating bands. Compared to the reference antenna array, the array with the metasurface structure exhibits reduction in sideband emissions. The discrepancy between simulated and measured results is due manufacturing tolerances and mismatch between the feedline and the antenna.

Decoupling effects can also be observed by visualizing the surface current distribution plots over the 2×2 antenna array. With meander line metasurface isolator strong current is induced on the patch antenna and MLS, as shown in Fig. 9, which clearly verifies the effectiveness of the meander line metasurface isolator in suppressing surface current wave interaction between the four patches.

(a) Simulated   (b) Measured
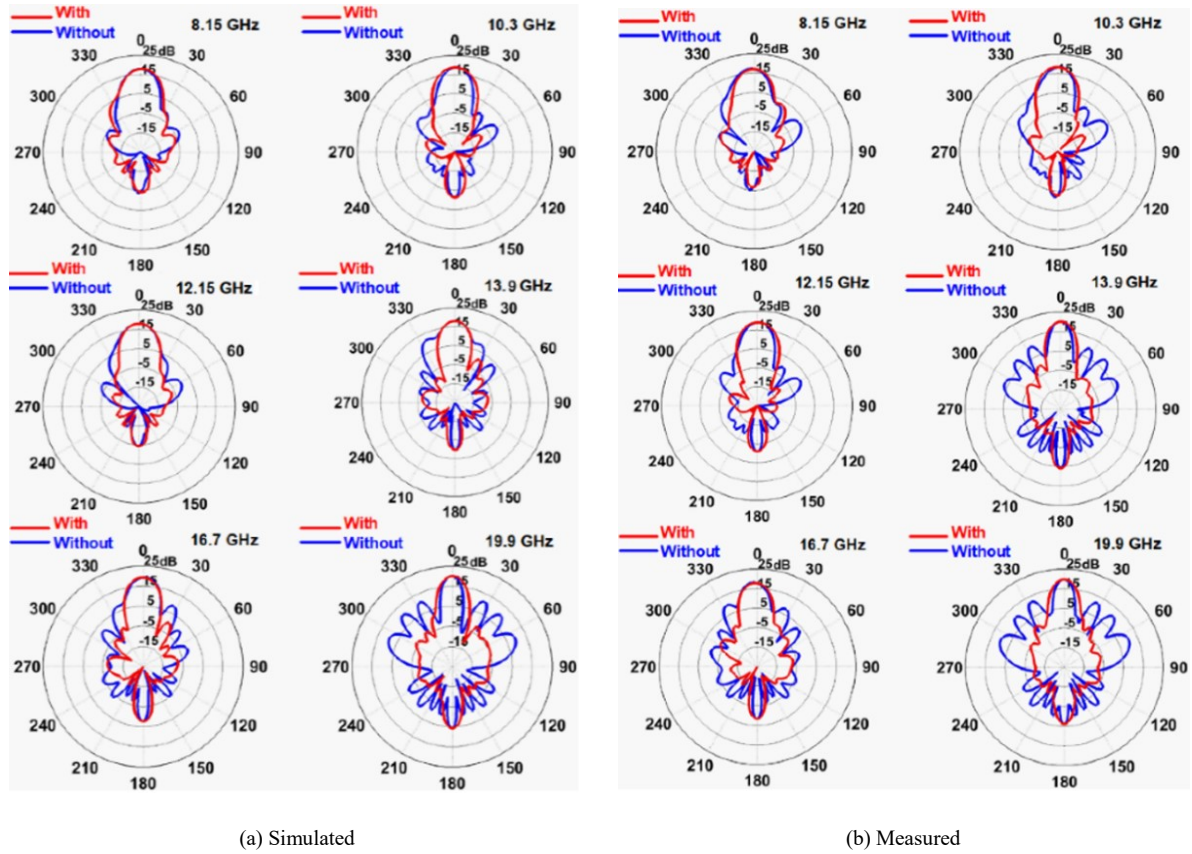
Fig. 8. Simulated and measured radiation patterns of the reference and proposed antenna arrays at various frequencies of 8.15, 10.3, 12.15, 13.9, 16.7, and 19.9 GHz.

(a) with no metasurface isolator @ 8.15 GHz   (b) with meander line metasurface isolator @ 8.15 GHz
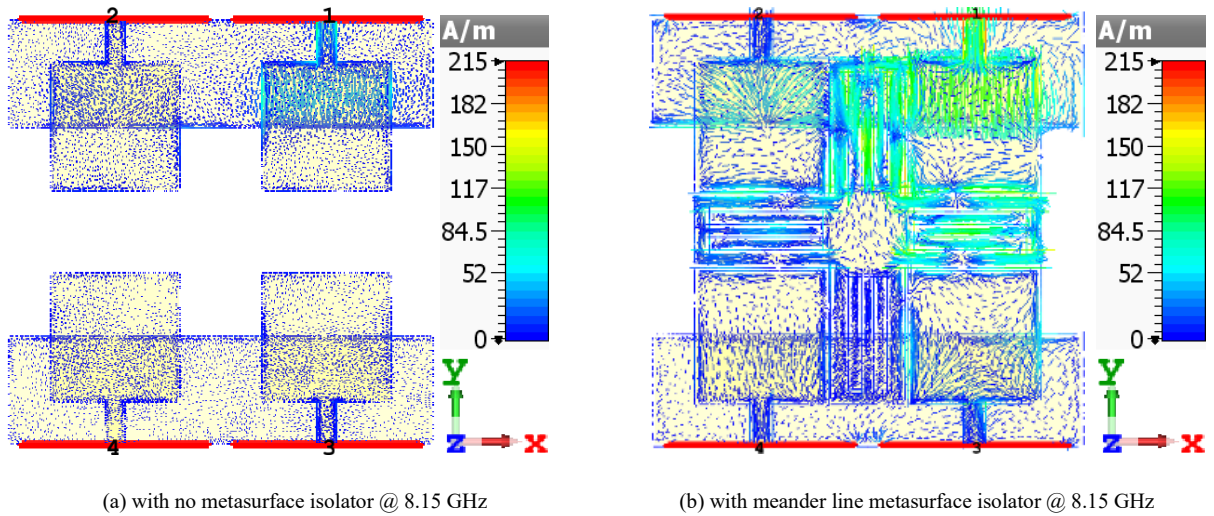
Fig.9. Surface current distribution at a spot frequency over the reference antenna array with no metasurface, and over the antenna array with meander line metasurface isolator.

5

The figure of merit for MIMO enabled antenna systems is represented by envelop correlation coefficient (ECC). It can be calculated from measured field patterns by using [12]

$$\rho_e = \frac{\left|\iint_{4\pi} \vec{E}_1(\theta,\phi) \cdot \vec{E}_2(\theta,\phi) d\Omega\right|^2}{\iint_{4\pi}\left|\vec{E}_1(\theta,\phi)\right|^2 d\Omega \cdot \iint_{4\pi}\left|\vec{E}_1(\theta,\phi)\right|^2 d\Omega} \qquad (1)$$

Where

$$\vec{E}_1(\theta,\phi) \cdot \vec{E}_2(\theta,\phi) = \vec{E}_{\theta 1}^*(\theta,\phi) \cdot \vec{E}_{\theta 2}^*(\theta,\phi) + \vec{E}_{\phi 1}^*(\theta,\phi) \cdot \vec{E}_{\phi 2}^*(\theta,\phi) \quad (2)$$

The term $\vec{E}_1(\theta,\phi)$ is the measured electric-field vector radiated by antenna#1 while other antenna ports are terminated with a 50Ω matched load [12]. The calculated ECCs for the array with and without metasurface are shown in Fig. 10. It is evident that by introducing the metasurface, the ECC has improved from 0.35 to less than 0.125. This should result in a higher channel capacity and diversity gain.
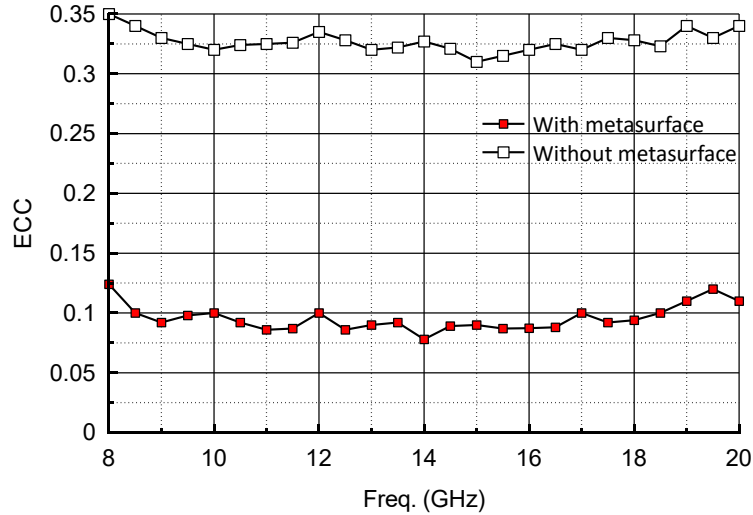

Fig.10. Envelop correlation coefficient (ECC) for the array with and without metasurface.

III. COMPARISON WITH LITERATURE

The proposed antenna array using metasurface is compared in Table III with other mutual coupling reduction techniques reported recently. Antenna arrays cited in Table III are: (i) constructed using two radiation elements; (ii) operate over a narrow and single band; (iii) employ defected ground structure (DGS); and (v) exhibit deteriorated radiation patterns. In this paper, we have increased the array elements to four to give a more accurate representation of an array. The proposed method described here offers an optimum isolation between adjacent antennas of 32 dB at X-band, 27 dB at Ku-band, and 26 dB at K-band, which is significantly better than the references cited with exception of [13]. In [13] the authors achieved very good isolation of 40 dB using short-circuited via-holes, which is not used in our case, however the antenna operates in a very narrow band. Also, close examination of the decoupling structure in [24] reveals it is based on interdigital capacitance structure not slotted meander line. Compared to the decoupling structure in [24] the proposed metasurface (i) enables large number of radiation elements to be arranged more compactly in a symmetrical configuration; (ii) exhibits a much wider impedance bandwidth of 5.4 GHz for return-loss better than -10 dB; and (iii) isolation improvement on average is 10 dB better over the operating range of the antenna. Furthermore, the proposed technique is simple to implement in practice and can be retrofitted to existing antenna arrays quickly and at low cost. It is important to mention that, to achieve high isolation with a simple structure, the proposed array antenna was realized on a truncated ground-plane. Unlike other techniques the proposed technique is relatively easy to design and implement in practice.

TABLE III. COMPARISON BETWEEN THE PROPOSED ARRAY WITH THE RECENT WORKS

Ref.	Method	Max. isolation	Bandwidth	Bands	Reduction in bandwidth	Rad. pattern deterioration	No. of elements	Use of DGS	Edge-to-Edge Gap
[2]	EBG	8.8 dB	Narrow	Single	Yes	-	2	Yes	$0.75\lambda_0$
[3]	Fractal load & DGS	16 dB	Narrow	Single	Yes	No	2	Yes	$0.22\lambda_0$
[4]	U-Shaped Resonator	10 dB	Narrow	Single	Yes	Yes	2	Yes	$0.6\lambda_0$
[6]	I-Shaped Resonator	30 dB	Narrow	Single	Yes	Yes	2	Yes	$0.45\lambda_0$
[7]	W/g MTM	18 dB	Narrow	Single	Yes	No	2	Yes	$0.093\lambda_0$
[13]	Ground Slot	40 dB	Narrow	Single	Yes	Yes	2	Yes	$0.23\lambda_0$
[14]	SCSRR	10 dB	Narrow	Single	Yes	Yes	2	Yes	$0.25\lambda_0$

[15]	SCSSRR	14.6 dB	Narrow	Single	Yes	Yes	2	Yes	$0.125\lambda_0$
[16]	Compact EBG	17 dB	Narrow	Single	Yes	Yes	2	Yes	$0.8\lambda_0$
[17]	Meander line	10 dB	Narrow	Single	Yes	No	2	Yes	$0.055\lambda_0$
[18]	UC-EBG	14 dB	Narrow	Single	Yes	Yes	2	Yes	$0.5\lambda_0$
[19]	EBG	10 dB	Narrow	Single	Yes	Yes	2	Yes	$0.5\lambda_0$
[20]	EBG	5 dB	Medium	Single	Yes	-	2	Yes	$0.6\lambda_0$
[21]	EBG	13 dB	Medium	Single	Yes	Yes	2	Yes	$0.5\lambda_0$
[22]	EBG&DGS	16 dB	Narrow	Single	Yes	No	2	Yes	$0.6\lambda_0$
[23]	EBG	4 dB	Narrow	Single	Yes	Yes	2	Yes	$0.84\lambda_0$
[24]	Slotted meander-line	16 dB	Narrow	Single	Yes	Yes	2	No	$0.11\lambda_0$
[25]	W/g MTM	20 dB	Narrow	Single	Yes	No	2	Yes	$0.125\lambda_0$
[26]	UC-EBG	10 dB	Narrow	Single	Yes	Yes	2	Yes	$0.5\lambda_0$
This work	Metasurface	32dB (X-band) 27dB (Ku-band) 26dB (K-band)	Cumulative BW is 5.4 GHz	Six	No	No	4	No	$0.26\lambda_0$

IV. CONCLUSION

A novel metasurface is shown to effectively isolate electromagnetic coupling between neighbouring antenna elements. Surface current waves over the patch antenna are suppressed by locating the cross-shaped metasurface between the radiating elements in the 2×2 antenna array. The proposed technique permits reduction in centre-to-centre separation between antenna radiating elements to $0.26\lambda_0$, where λ_0 is 8.0 GHz, does not require short-circuited via-holes or defected ground structures, and can be retrofitted. Over its operating range the proposed technique offers an optimum isolation between adjacent antennas of 32 dB at X-band, 27 dB at Ku-band, and 26 dB at K-band. The technique presented enables implementation of densely packed antenna arrays in MIMO and SAR systems.

REFERENCES

[1] A. Ludwig, "Mutual coupling, gain and directivity of an array of two identical antennas," IEEE Trans. Antennas Propag., vol.42, no. 6, 1976, pp. 837–841.

[2] F. Yang, and Y. Rahmat-Samii, "Microstrip antennas integrated with electromagnetic band-gap (EBG) structures: A low mutual coupling design for array applications," IEEE Trans. Antennas Propag., vol.51, no. 10, 2003, pp. 2936–2946.

[3] X. Yang, Y. Liu, Y.-X. Xu, and S.-X. Gong, "Isolation enhancement in patch antenna array with fractal UC-EBG structure and cross slot", IEEE Antennas Wireless Propag. Lett., vol. 16, 2017, pp. 2175-2178.

[4] M. T. Islam, and M. S. Alam, "Compact EBG structure for alleviating mutual coupling between patch antenna array elements," Progress in Electromagnetics Research, vol. 137, 2013, pp. 425-438.

[5] C. Y. Chiu, C. H. Cheng, R. D. Murch, and C. R. Rowell, "Reduction of mutual coupling between closely-packed antenna elements," IEEE Trans. Antennas Propag., vol.55, no. 6, 2007, pp. 1732–1738.

[6] C. K. Ghosh, and S. K. Parui, "Reduction of mutual coupling between E-shaped microstrip antennas by using a simple microstrip I-section," Microwave and Optical Tech. Lett., vol.55, no. 11, 2013, pp. 2544-2549.

[7] Z. Qamar, H.-C. Park, "Compact waveguided metamaterials for suppression of mutual coupling in microstrip array," Progress in Electromagnetics Research, vol. 149, 2014, pp. 183–192.

[8] Marco Faenzi, Gabriele Minatti, David González-Ovejero, Francesco Caminita, Enrica Martini, Cristian Della Giovampaola, and Stefano Maci, "Metasurface antennas: new models, applications and realizations," Scientific Reports, vol. 9, Article number: 10178, 2019, pp.1-14.

[9] Loïc Bernard, Mario Martinis, Sylvain Collardey, Kouroch Mahdjoubi, and Ronan Sauleau, "Metasurface antennas embedded in small circular cavities for telemetry applications," Applied Sciences. vol. 9, issue 12, 2019.

[10] D. Gonzalez Ovejero, X. Morvan, N. Chahat, G. Chattopadhyay, R. Sauleau, M. Ettorre, "Metallic metasurface antennas for space," 12th European Conference on Antennas and Propagation (EuCAP 2018), 2018.

[11] Feng Han Lin, Teng Li, and Zhi Ning Chen, "Recent progress in metasurface antennas using characteristic mode analysis," 13th European Conference on Antennas and Propagation (EuCAP), 31 March-5 April 2019, Krakow, Poland.

[12] Vaughan, R. G. & Andersen, J. B., "Antenna diversity in mobile communications," IEEE Trans. Veh. Technol., vol. 36, no.4, 1987, pp. 147–172.

[13] J. OuYang, F. Yang, and Z. M. Wang, "Reduction of mutual coupling of closely spaced microstrip MIMO antennas for WLAN application," IEEE Antennas Wireless Propag. Lett., vol. 10, 2011, pp. 310-312.

[14] F. G. Zhu, J. D. Xu, and Q. Xu, "Reduction of mutual coupling between closely packed antenna elements using defected ground structure," Electronics Letters, vol. 45, no. 12, pp. 601–602, 2012.

[15] M. M. B. Suwailam, O. F. Siddiqui, and O. M. Ramahi, "Mutual coupling reduction between microstrip patch antennas using slotted-complementary split-ring resonators," IEEE Antennas Wireless Propag. Lett., vol. 9, pp. 876–878, 2010.

[16] M. F. Shafique, Z. Qamar, L. Riaz, R. Saleem, and S. A. Khan, "Coupling suppression in densely packed microstrip arrays using metamaterial structure," Microwave and Optical Technology Letters, vol. 57, No. 3, pp. 759–763, 2015.

[17] S. Farsi, D. Schreurs, and B. Nauwelaers, "Mutual coupling reduction of planar antenna by using a simple microstrip U-section," IEEE Antennas Wireless Propag. Lett., vol. 11, pp. 1501-1503, 2012.

[18] J. Ghosh, S. Ghosal, D. Mitra, and S. Ranjan B. Chaudhuri, "Mutual coupling reduction between closely placed microstrip patch antenna using meander line resonator," Progress in Electromagnetic Research Letters, vol. 59, pp. 115–122, 2016.

[19] H. S. Farahani, M. Veysi, M. Kamyab, and A. Tadjalli, "Mutual coupling reduction in patch antenna arrays using a UC-EBG superstrate," IEEE Antennas Wireless Propag. Lett., vol. 9, pp. 57–59, 2010.

[20] E. Rajo-Iglesias, O. Quevedo-Teruel, and L. Inclan-Sanchez, "Mutual coupling reduction in patch antenna arrays by using a planar EBG structure and a multilayer dielectric substrate," IEEE Trans. Antennas Propag., vol. 56, no. 6, pp. 1648–1655, Jun. 2008.

[21] M. J. Al-Hasan, T. A. Denidni, and A. R. Sebak, "Millimeter wave compact EBG structure for mutual coupling reduction applications," IEEE Trans. Antennas Propag., vol. 63, no. 2, pp. 823–828, Feb. 2015.

[22] G. Exposito-Dominguez, J. M. Fernandez-Gonzalez, P. Padilla, and M. Sierra-Castaner, "Mutual coupling reduction using EBG in steering antennas," IEEE Antennas Wireless Propag. Lett., vol. 11, pp. 1265–1268, 2012.

[23] A. Yu, and X. Zhang, "A novel method to improve the performance of microstrip antenna arrays using a dumbbell EBG structure," IEEE Antennas Wireless Propag. Lett., vol. 2, No. 1, pp. 170–172, 2003.

[24] M. G. Alsath, M. Kanagasabai, and B. Balasubramanian, "Implementation of slotted meander line resonators for isolation enhancement in microstrip patch antenna arrays," IEEE Antennas Wireless Propag. Lett., vol. 12, pp. 15–18, 2013.

[25] X. M. Yang, X. G. Liu, X. Y. Zhu, and T. J. Cui, "Reduction of mutual coupling between closely packed patch antenna using waveguide metamaterials," IEEE Antennas Wireless Propag. Lett., vol. 11, pp. 389-391, 2012.

[26] H. S. Farahani, M. Veysi, M. Kamyab, and A. Tadjalli, "Mutual coupling reduction in patch antenna arrays using a UC-EBG superstate," IEEE Antennas Wireless Propag. Lett., vol. 9, pp.57-59, 2010.